WS02-D02

4D Reservoir Analysis beyond 1D Convolutions

A. Khalil* (CGG), H. Hoeber (CGG), A. Jafargandomi (CGG) & S. de Pierrepont (CGG)

SUMMARY

Analysis of time-lapse data is performed on migrated seismic images, which represent the spatial and time-lapse variability of the medium's reflectivity. The process of migration effectively rotates the wavelet so that it is normal to the imaged reflectors. Processes used in 4D reservoir analysis such as deconvolution, inversion and warping need to follow the structure of the data. The traditional 1D (vertical) convolutional approach does not honour this directivity. For this reason, we introduce a wave equation based approach which provides an effective platform for structurally consistent reservoir analysis. This includes applications such as wavelet extraction, warping and 4D time-strain inversion.

Introduction

A migrated seismic image represents the spatial variability of the earth's reflectivity. The process of migration effectively rotates the seismic wavelet so that it is normal to the imaged reflectors. In the presence of complex geologies and steep dips, the wavelet, when viewed vertically, is stretched according to the structural dip of the image.

Time-lapse analysis methods that attempt to invert changes observed on the migrated images of base and monitors for velocity and impedance generally assume vertical propagation (1D convolution). In dipping and complex media, this assumption no longer holds, as time-strain changes propagate normal to the reflectors (Thore *et al*., 2012; Audebert and Agut, 2014).

We reintroduce the concept of seismic image waves, originally proposed by Hubral *et al*. (1996), to define an image wave equation. The wavefield solution of this wave equation allows us to perform kinematic and amplitude inversions of time-lapse data on dipping and complex structures. The method is applicable to pre- and post-stack data and is easily combined with existing time and amplitude inversion methods.

Theory

Seismic data is recorded at the surface of the acquisition survey where amplitude variation with respect to time is measured. Imaging algorithms map the energy recorded on the surface back to the subsurface locations which generated the reflections. The wavelet is then everywhere normal to the reflectors. Figure 1 shows schematically the wavelets for a simple dipping event before and after imaging. Conceptually, pre-imaging, the wavelets are aligned with the time axis, while post-imaging they are orthogonal to the reflector and depth variations are stretched by the dip.

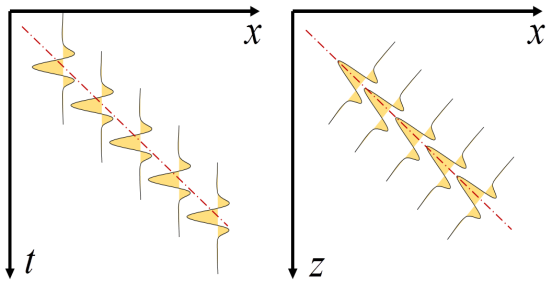

Figure 1 *The seismic wavelet for pre-imaging (left) and post-imaging (right) data.*

Multiple attempts have been made to remove the effect of this stretch. In a coloured inversion (Lancaster and Whitcombe, 2000) context, Lazaratos and David (2009) apply the shaping operators pre-imaging. More recently Cherrett (2013) proposed a frequency-wavenumber approach for modelling and inversion; this method assumes a constant velocity.

From a time-lapse perspective, as pointed out by Thore *et al*. (2012) and Audebert and Agut (2014), 4D changes propagate in the direction normal to the reflectors. This limits the applicability of 1D post-imaging methods and points towards pre-imaging approaches such as time-lapse (4D) full waveform inversion (FWI), as proposed by Asnashaari *et al*. (2011). FWI would of course be ideal, but it is computationally expensive and difficult to control as it operates on pre-imaging data.

Our solution lies mid-way between the complex pre-imaging and simplistic post-imaging paradigms. We reintroduce the concept of a seismic image wave (Hubral *et al*., 1996), by positing that a seismic image follows a wave equation of the form

$$\frac{1}{v^2(\underline{\mathbf{x}})}\partial_\tau^2 I(\underline{\mathbf{x}};\tau) = \nabla^2 I(\underline{\mathbf{x}};\tau) \quad , \quad v(\underline{\mathbf{x}}) = \frac{1}{2}\frac{c(\underline{\mathbf{x}})}{\cos(\theta)} \quad , \tag{1}$$

where $\underline{\mathbf{x}} = (x, y, z)$ is the space coordinate vector, τ is a time-like coordinate, $c(\underline{\mathbf{x}})$ is the velocity of the medium, θ is the reflection angle, and $I(\underline{\mathbf{x}};\tau)$ is the seismic image wavefield associated with this reflection angle, i.e., a common-angle seismic image.

We derive Equation 1 using the cross-correlation imaging principle. This relationship is not new to the seismic literature: it has existed for a long time in different forms. Typically, the Fourier representation is used, as for example in Sava and Fomel (2006). Mosher *et al*. (1996) derive a similar relation for a common-angle time migration scheme, and Zhang and Sun (2009) use it to remove low frequency artefacts from reverse-time migration in what is commonly known as the 'Laplacian' process.

As with any wave equation, a wavefield solution is computed by defining initial and boundary conditions. In our implementation we set the zero time of the seismic image wavefield to the input seismic image $I_o(\underline{\mathbf{x}})$

$$I(\underline{\mathbf{x}};\tau=0)=I_o(\underline{\mathbf{x}}) \quad . \tag{2}$$

Then we solve $I(\underline{\mathbf{x}};\tau)$ for an arbitrary range of τ using methods such as finite-differences or pseudo-spectral schemes.

By definition, the τ axis is orthogonal to the wavefield which encompasses imaged reflectors. It therefore captures physical changes in a structurally consistent way. This axis serves as our domain of analysis for 4D effects. To emphasize the orthogonality property and to discriminate τ from the vertical time, we refer to this axis as orthogonal time. Figure 2 shows a cartoon demonstrating this concept.

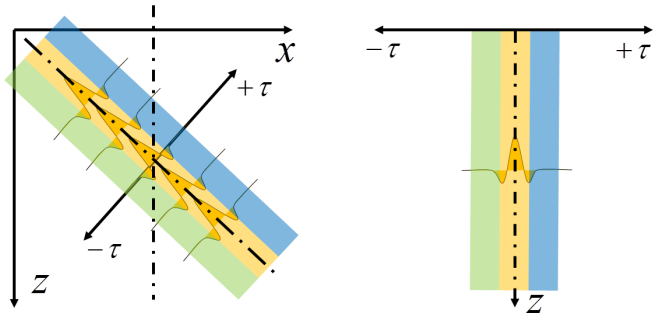

Figure 2 *A dipping reflector and the direction of orthogonal time (left). The corresponding gather along the orthogonal time axis (right).*

Wavelet extraction

Before turning to 4D analysis we illustrate the use of the orthogonal time axis in the context of wavelet extraction. We start by imaging two simple linear events, one flat, and the other dipping by 20°. Both events are convolved with the same wavelet. After imaging we extract the wavelets from migrated data, first along the traditional vertical time axis (after depth-to-time conversion of the PSDM image); and secondly along the orthogonal time axis generated with the proposed method.

Figure 3 shows all four wavelets obtained. The top image superposes the two wavelets obtained with the 1D convolutional approach. The extracted wavelets differ since the dip of the structure is not accounted for with this method. A 1D convolutional inversion with a stationary wavelet is biased by this effect, as it effectively sees the wavelet change with dip. The lower part of Figure 3 shows the two wavelets (flat event and dipping event) we extract along the orthogonal time axis. The wavelets are the same, showing that inversion along this direction can be done with a single stationary wavelet.

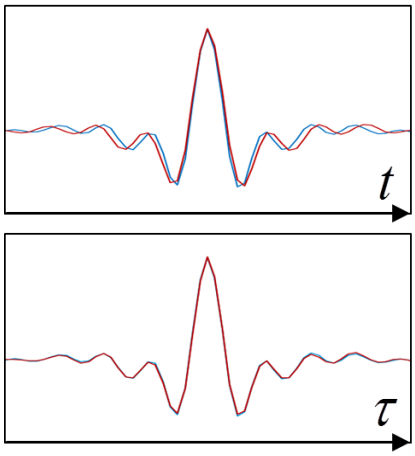

Figure 3 *Wavelets for a flat (blue) and a dipping (red) event, extracted along the traditional vertical time (top) and along the orthogonal time (bottom).*

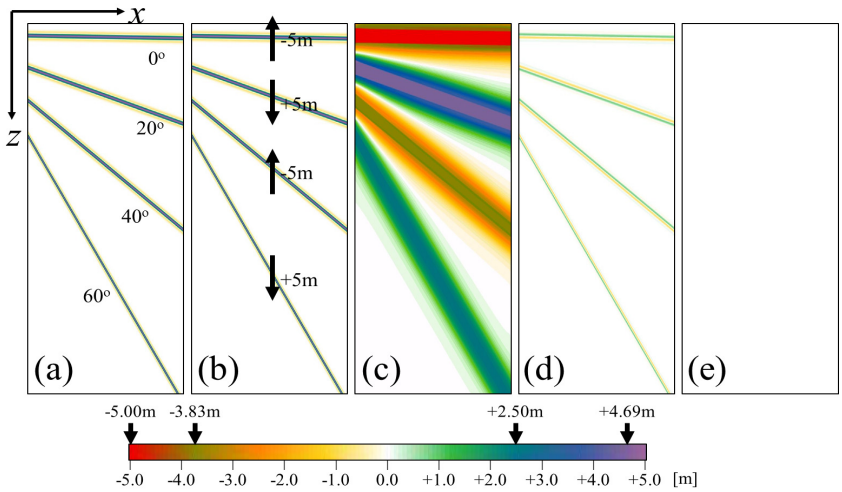

Figure 4 *A synthetic dataset composed of four dipping layers. (a) The base dataset. (b) The monitor dataset, generated by applying positive and negative 5m shifts in the vertical direction. (c) The estimated normal displacements; they correctly match theoretical values. (d) The difference between base and monitor datasets. (e) The difference after applying the estimated shifts.*

Time-shift and time-strain analysis

In Figure 4 we construct a synthetic test data with four dips and we apply vertical shifts of plus or minus five metres to all events. The shifts extracted along the orthogonal axis are correctly estimated matching theoretical values i.e. the vertical displacement multiplied by the cosine of the dip angle.

Figure 5 shows a realistic synthetic seismic example, where the monitor data is injected with a small 4D velocity change, inducing the time-shift. We then use the image wave equation to generate the orthogonal time axis which is used for time-shift and -strain analysis. Reservoir analysis algorithms such as kinematic or amplitude inversions can now be performed along this dimension. This can be done on full stacks or on pre-stack angle gathers. Figure 6 shows the results for the estimated time-shifts using the traditional vertical as well as orthogonal time. Using the traditional vertical time method the changing reflector dips with depth induce an unphysical time-shift gradient effect. This happens because the process is not following the propagation wave-front consistently. Using the orthogonal axis the time-shift attribute appears more homogenous and aligned with the reflectors' directions. This effect has an impact on the time-strain attribute (Figure 7): For the vertical case, the strain attribute indicates a false velocity change below deeper dipping events. By contrast, the time-strain obtained along orthogonal time correctly identifies the location of the velocity change on the shallower (flat) event. This demonstrates that 1D convolutional analysis can potentially cause false interpretations.

Conclusions

In complex non-flat structures, imaging and reservoir processing algorithms designed to analyse 4D effects must honour the direction of energy propagation normal to the dips. Our wave equation based approach, utilizing the orthogonal time axis, provides an effective way to use existing 4D analysis techniques, pre- or post-stack. The method is relatively simple and fast to implement, cheaper than FWI, and more general than existing stationary techniques in frequency-wavenumber domain.

Acknowledgments

We thank CGG's management and the Multi-Client-New-Ventures division for permission to publish and show the seismic data, and our colleagues in CGG and in the BP DPC Aberdeen for useful discussions.

References

Asnaashari, A., Garambois, S., Audebert, F., Thore, P., and Virieux, J. [2011] Sensitivity analysis of time-lapse images obtained by differential waveform inversion with respect to reference model: *81st Annual International Meeting, SEG*, Expanded Abstracts, 2482–2486.

Audebert, F. and Agut, C. [2014] Making time-domain "warping" applicable to the retrieval of 4D perturbations in depth imaging contexts: *84th Ann. Intern. Meeting, SEG*, Expanded Abstracts.

Cherrett, A. [2013] Dip correction for Convolutional Modelling and Elastic Inversion: *75th EAGE Conference and Exhibition*, Extended Abstracts, Tu 10 13.

Hubral, P., Tygel, M., and Schleicher, J. [1996] Seismic image waves: *Geophysical Journal International*, **125**, 431-442.

Lancaster, S., and Whitcombe, D. [2000] Fast track 'Coloured' inversion: *SEG Technical Program* Expanded Abstracts, 1572–1575.

Lazaratos, S., and David, R. L. [2009] Inversion by pre-migration spectral shaping: *SEG Technical Program* Expanded Abstracts, 2383-2387.

Mosher, C. C., Keho T. H., Weglein, A. A., and Foster, D. J. [1996] The impact of migration on AVO: *Geophysics*, **61**(6), P1603-1615.

Sava, P., and Fomel, S. [2006] Time-shift imaging condition in seismic migration: *Geophysics*, **71**(6), S209-S217.

Thore, P., Verdiere, C. De., and McManus, E. [2012] Estimation of 4D signal in complex media, A fast track approach: *82nd Annual International Meeting, SEG*, Expanded Abstracts.

Zhang, Y., and Sun, J. [2009] Practical issues in reverse time migration: true amplitude gathers, noise removal and harmonic source encoding: *First Break*, **27**(1), 53-59.

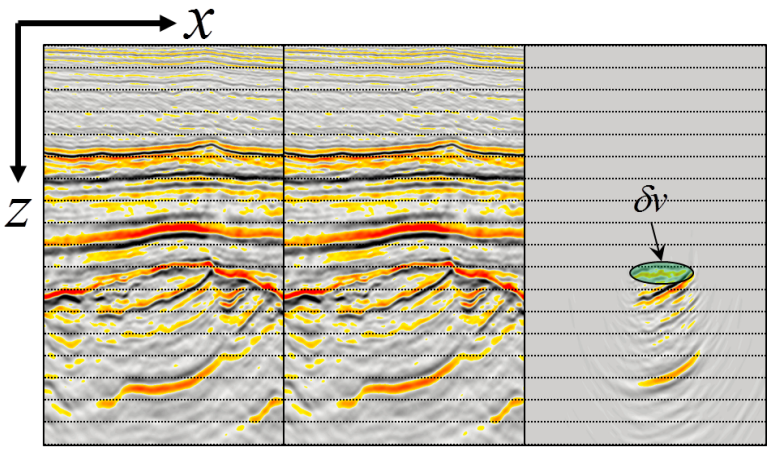

Figure 5 *Base and monitor datasets (left and middle). The monitor dataset is generated by inducing a velocity change within the area of the oval to give the 4D difference on the right.*

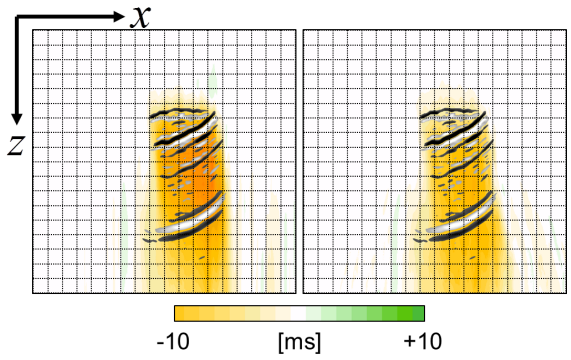

Figure 6 *Estimated 4D time-shift, using the traditional vertical time (left) and using orthogonal time (right).*

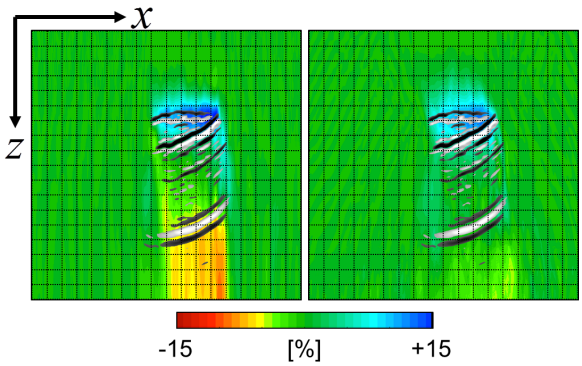

Figure 7 *Estimated 4D time-strain, using the traditional vertical time (left) and using orthogonal time (right).*